Recent developments in the field of colloidal dispersions in nematic liquid crystals: the Stokes drag

2003 J. Phys.: Condens. Matter 15 S191

(http://iopscience.iop.org/0953-8984/15/1/324)

INSTITUTE OF PHYSICS PUBLISHING JOURNAL OF PHYSICS: CONDENSED MATTER

J. Phys.: Condens. Matter **15** (2003) S191–S196 PII: S0953-8984(03)54889-5

Recent developments in the field of colloidal dispersions in nematic liquid crystals: the Stokes drag

Holger Stark, Dieter Ventzki and Michael Reichert

Universität Konstanz, Fachbereich Physik, Fach M621, D-78467 Konstanz, Germany

E-mail: Holger.Stark@uni-konstanz.de

Received 16 October 2002
Published 16 December 2002
Online at stacks.iop.org/JPhysCM/15/S191

Abstract

We review the novel features of the Stokes drag of a spherical particle dispersed in a nematic solvent. It is anisotropic, couples to rotations of the particle, and exhibits strong non-linearities.

In recent years, colloidal dispersions in nematic liquid crystals have emerged as a novel type of soft matter (for a review see [1]). The fast development of the field started after the ground-breaking work of Poulin *et al* on nematic emulsions [2], although earlier experimental [3, 4] and theoretical [5] work revealed some of the fascinating facets of the new system. The long-range orientational order in the nematic phase, with its possibility of elastic distortions and the occurrence of topological defects, gives rise to interesting new features of the novel colloidal state. A careful study of the director configurations around a single particle, with rigid radial anchoring of the molecules at the surface and uniform alignment at infinity, revealed two characteristic structures (see figure 1): the dipole configuration with a topological point defect attached to the particle and the Saturn-ring configuration where a $-1/2$ disclination ring encircles the particle at the equator [1]. New interactions arise (see [1] for a review) even above the nematic–isotropic phase transition [6], and prominent structure formation is observed, including chaining [7], gel-like ordering with viscoelastic properties [8], and even ordered particle arrays [9]. Several advanced numerical methods are applied in the study of nematic colloids including the simulation of multi-particle systems [10], adaptive grids [11], and lattice Boltzmann simulations [12].

In this contribution, we address the Stokes drag—a dynamic quantity whose careful analysis always has to be performed at the outset when the dynamics of multi-particle systems is studied. The Stokes drag of particles in a nematic solvent has some history, summarized in [1]. The first realistic calculations are due to Ruhwandl and Terentjev [13] who concentrated on the Saturn-ring configuration. Their work was extended to the more interesting dipole configuration by Stark and Ventzki [14] who also relaxed the constraint of a fixed director field, treating its dynamics explicitly [15]. In the following, we summarize recent results and add new insights. The novelties of the Stokes drag in a nematic solvent are threefold. First,

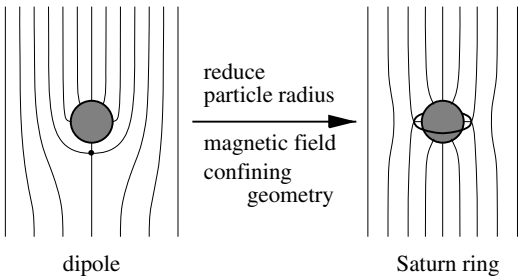

Figure 1. Two possible director configurations for a spherical particle in a nematic environment with uniform director field at infinity. The molecules are radially anchored at the surface of the particle. The point defect in the dipole configuration can be opened up to a $-1/2$ disclination ring encircling the equator of the sphere. This transition occurs when the particle radius is decreased (keeping the radial anchoring), a magnetic or electric field is applied, or the particle is strongly confined.

it is anisotropic, which offers the possibility of lift forces. Secondly, a coupling between translational and rotational motion occurs which does not exist in simple isotropic fluids for spherical particles [16]. Thirdly, the Stokes drag is highly non-linear. Before we address these features in detail, we start with a short review of the Stokes drag in an isotropic fluid followed by an explanation of the Ericksen–Leslie equations, which describe the dynamics of nematic liquid crystals.

A particle of radius a moving with velocity v_0 in an isotropic fluid of shear viscosity η experiences the well-known Stokes drag force, $F_S = 6\pi\eta a v_0$ [17]. To calculate this force, one can also look at a fluid flowing around a particle at rest with a velocity $\boldsymbol{v}_\infty$ at infinity and the non-slip boundary condition ($\boldsymbol{v} = \boldsymbol{0}$) at the particle surface. The velocity and pressure (p) fields follow from the incompressibility condition and the momentum balance:

$$\operatorname{div} \boldsymbol{v} = 0, \qquad -\boldsymbol{\nabla} p + \operatorname{div} \boldsymbol{\sigma}^{\mathrm{visc}} = \boldsymbol{0}, \tag{1}$$

where $\sigma_{ij}^{\mathrm{visc}} = 2\eta A_{ij} = \eta(\nabla_i v_j + \nabla_j v_i)$ stands for the viscous stress tensor in an isotropic fluid, and the Reynolds number is chosen small enough that the convective term, $\boldsymbol{v} \cdot \boldsymbol{\nabla} \boldsymbol{v}$, can be neglected. Integrating the total stress tensor including the pressure over the particle surface results in the known Stokes friction coefficient $\gamma = 6\pi\eta a$.

In order to calculate the Stokes drag in a nematic solvent, we have to solve the Ericksen–Leslie equations which are commonly used to described the dynamics of a nematic liquid crystal [18, 19]. The formal structure of the momentum balance equation (1) is still valid; however, the viscous stress tensor has to be replaced by a more complicated object: $\boldsymbol{\sigma}^{\mathrm{visc}} \to \boldsymbol{\sigma}^{\mathrm{el}} + \boldsymbol{\sigma}^{\mathrm{visc}}$, where

$$\sigma_{ij}^{\mathrm{el}} = -\frac{\partial f_{\boldsymbol{n}}}{\partial \nabla_j n_k} \nabla_i n_k \tag{2}$$

$$\sigma_{ij}^{\mathrm{visc}} = \alpha_4 A_{ij} + \alpha_1 n_i n_j n_k n_l A_{kl} + \alpha_5 n_j n_k A_{ik} + \alpha_6 n_i n_k A_{jk} + \alpha_2 n_j N_i + \alpha_3 n_i N_j. \tag{3}$$

An elastic contribution $\boldsymbol{\sigma}^{\mathrm{el}}$ to the stress tensor appears which is due to elastic distortions of the director field described quantitatively by the Frank free energy. In the one-constant approximation, it reads $f_{\boldsymbol{n}} = K(\nabla_i n_j)^2/2$, where K is the Frank elastic constant. The viscous stress tensor $\boldsymbol{\sigma}^{\mathrm{visc}}$ with the Leslie viscosities α_i contains of course the isotropic term but, in addition, the strain rate $\boldsymbol{A}$ also couples to the director due to the local uniaxial symmetry of a nematic. According to these terms, several Mięsowicz shear viscosities exist depending on the explicit shear geometry [20]. Two further terms in the viscous stress tensor contain the rate of change of the director relative to a fluid vortex: $\boldsymbol{N} = \partial \boldsymbol{n}/\partial t + \boldsymbol{v} \cdot \boldsymbol{\nabla} \boldsymbol{n} - \operatorname{curl} \boldsymbol{v} \times \boldsymbol{n}/2$. In the

second dynamic equation, which governs the temporal evolution of the director field $\boldsymbol{n}(\boldsymbol{r}, t)$, elastic and viscous torques are balanced: $\boldsymbol{n} \times \boldsymbol{h}^{\mathrm{el}} = \boldsymbol{n} \times \boldsymbol{h}^{\mathrm{visc}}$, where

$$h_i^{\mathrm{el}} = \nabla_j \frac{\partial f_{\boldsymbol{n}}}{\partial \nabla_j n_i} - \frac{\partial f_{\boldsymbol{n}}}{\partial n_i} \qquad \text{and} \qquad h_i^{\mathrm{visc}} = \gamma_1 N_i + \gamma_2 A_{ij} n_j. \tag{4}$$

In the static case, the director field is determined by $\boldsymbol{n} \times \boldsymbol{h}^{\mathrm{el}} = \boldsymbol{0}$. The coefficient γ_1 in $\boldsymbol{h}^{\mathrm{visc}}$ denotes a true rotational viscosity of the director motion. It contributes to the viscous torque even in the stationary case whenever $\boldsymbol{\nabla n} \neq \boldsymbol{0}$. Onsager relations require a connection to the Leslie viscosities: $\gamma_1 = \alpha_3 - \alpha_2$ and $\gamma_2 = \alpha_2 + \alpha_3 = \alpha_6 - \alpha_5$ [18, 19]. The origin of $\boldsymbol{n} \times (\boldsymbol{h}^{\mathrm{el}} - \boldsymbol{h}^{\mathrm{visc}}) = \boldsymbol{0}$ is controversial in the derivation of Ericksen and Leslie. Based on microscopic Poisson brackets and the formalism developed for stochastic equations, the Ericksen–Leslie equations became rigorously derivable quite recently [21].

Finally, the Stokes drag on the sphere is calculated by integrating the complete stress tensor over the surface of the sphere: $\boldsymbol{F}_S = \int_S (-p\boldsymbol{1} + \boldsymbol{\sigma}^{\mathrm{el}} + \boldsymbol{\sigma}^{\mathrm{visc}})\, \mathrm{d}\boldsymbol{S}$, where the surface element $\mathrm{d}\boldsymbol{S}$ is a vector directed towards the fluid. An alternative calculation of the Stokes drag via the dissipation function is also possible [14, 15]. The viscous torque on the sphere follows from $\boldsymbol{M} = \int_S \boldsymbol{r} \times (-p\boldsymbol{1} + \boldsymbol{\sigma}^{\mathrm{el}} + \boldsymbol{\sigma}^{\mathrm{visc}})\, \mathrm{d}\boldsymbol{S}$.

The momentum balance and the torque equation were solved numerically via the Newton–Gauss–Seidel method. To determine the pressure, the method of artificial compressibility was used. Depending on the symmetry of the problem, either two- or three-dimensional calculations with different integration volumes have to be performed. The numerics of these equations is generally quite complex and needs a careful treatment of the boundary conditions. Details are given in [14, 15].

The solutions of the Ericksen–Leslie equations are non-trivial. However, we can categorize them by introducing the Ericksen number Er in analogy to the Reynolds number. The Ericksen number gives an estimate for the ratio of frictional to elastic forces in the nematic liquid crystal, i.e., $Er = \alpha_4 v_\infty a/(2K)$, where, generally, v_∞ and a denote a characteristic velocity and length scale of the system, respectively. In the limit of small Ericksen numbers, $Er \ll 1$, we can neglect the response of the director field to the flow field and just use the static director field for $\boldsymbol{v} = \boldsymbol{0}$. (For a critical remark about this approximation, see [14].) We are left with the solution of the momentum balance where it can be shown that the elastic stress tensor $\boldsymbol{\sigma}^{\mathrm{el}}$ of equation (2) renormalizes the pressure, so only the viscous stress tensor $\boldsymbol{\sigma}^{\mathrm{visc}}$ of equation (3) has to be taken into account (see [14]).

In the case of low Ericksen numbers, the momentum balance is linear in the velocity field and the director field does not contribute to the dynamics. This implies a linear relation between the Stokes force and the velocity $\boldsymbol{v}_\infty$. The dipole or Saturn-ring configuration or just a uniform director field, in which a particle is immersed, exhibit an overall uniaxial symmetry say along the z-axis. Then, in general, the Stokes force will not point along $\boldsymbol{v}_\infty$; we have to introduce the friction tensor $\boldsymbol{\gamma}$:

$$\boldsymbol{F}_S = \boldsymbol{\gamma} \boldsymbol{v}_\infty \qquad \text{with } \boldsymbol{\gamma} = \gamma_\perp \boldsymbol{1} + (\gamma_\parallel - \gamma_\perp)\hat{\boldsymbol{z}} \otimes \hat{\boldsymbol{z}}, \tag{5}$$

where $\hat{\boldsymbol{z}}$ is the unit vector along the z-axis, and $\gamma_\parallel$, $\gamma_\perp$ denote, respectively, the friction coefficient along and perpendicular to $\hat{\boldsymbol{z}}$. Such a form of the friction tensor allows drift or lift forces acting perpendicular to $\boldsymbol{v}_\infty$ [13]. For example, let a particle fall in a nematic solvent with the overall symmetry axis inclined against the vertical direction; then the particle will drift along the horizontal direction. We have determined $\gamma_\parallel$ and $\gamma_\perp$ for the three configurations mentioned above and the two nematic compounds MBBA and 5CB. We find that the ratio $\gamma_\perp/\gamma_\parallel$ lies between 1.5 and 2.0 which should be measurable in an experiment. Furthermore, we observe that the dipole and Saturn-ring configurations possess similar ratios whereas for a uniform director field the ratio is larger by 20% [14].

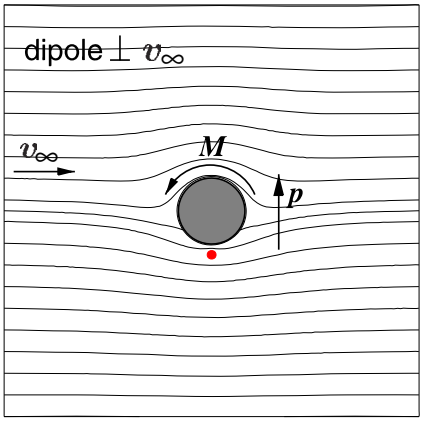

Figure 2. The streamline pattern for the dipole configuration oriented perpendicular to v_∞. The point defect is indicated by the dot below the sphere. A non-zero viscous torque $M \propto p \times v_\infty$ induces an anticlockwise rotation of the particle.

(This figure is in colour only in the electronic version)

In the following we discuss further special features of the Stokes drag. In figure 2 we plot the streamline pattern of the velocity field for v_∞ perpendicular to the dipolar axis. The point defect in the director field is indicated by a dot. The missing mirror plane of the dipole configuration is clearly recognizable, and the point defect gives rise to a dip in one of the streamlines. Although the pattern resembles that of the Magnus effect [22], symmetry dictates that the Stokes drag $F_S^\perp \parallel v_\infty$ (see equation (5)). A lift force perpendicular to v_∞ cannot exist so far. However, in our numerical calculations, we find a non-zero viscous torque M acting on the particle whose direction for a fluid flow from left to right is indicated in figure 2. Symmetry allows such a torque M since the cross-product of a dipole moment p, which can be assigned to the dipolar configuration (see [2, 23]), and v_∞ gives an axial vector or pseudovector, $M \propto p \times v_\infty$. In the Saturn-ring configuration a non-zero dipole moment cannot exist by symmetry, and therefore a non-zero torque does not occur. We had to correct the direction of the torque in figure 2 from that in our earlier publication [14]. Now the direction of M seems to be counterintuitive, since according to the streamline pattern more surface of the sphere is exposed to shear stresses acting from left to right. On the other hand, the director field around the defect produces a high resistance for the flow field via the complex viscous stress tensor, which is then transferred to the particle surface and might therefore explain the direction of M. The torque M induces a rotation of the particle which we took into account in our numerical calculations by changing the boundary condition of the velocity field at the particle's surface. We ultimately find an angular velocity Ω where the torque M vanishes. Now, in principle, a Magnus force proportional to $v_\infty \times \Omega$ is also allowed acting perpendicular to v_∞ and Ω. However, such a force is beyond our theory linearized in V. To illustrate that our observations are not at all trivial, let us compare them to the Stokes drag in isotropic fluids. Detailed investigations of Brenner [16] show that spherical particles or, more generally, particles which are non-chiral in the sense that they coincide with their mirror picture just fall under the influence of gravity without rotating. From what we learnt above about a nematic solvent, we deduce that a spherical particle will start to spin about a horizontal axis when it is surrounded by the dipolar director configuration which is also oriented along the horizontal. Such an effect should clearly be observable in experiments.

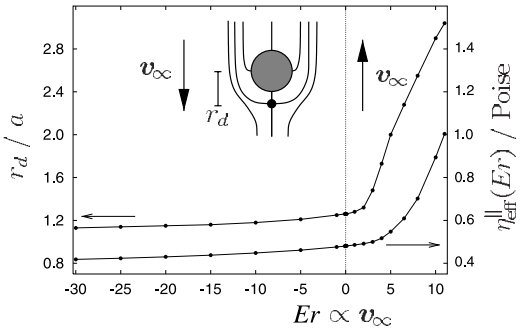

Figure 3. For the dipole configuration, the distance r_d (between the point defect and the centre of the sphere) and the effective viscosity $\eta^{\parallel}_{\rm eff}$ of the Stokes drag are plotted as a function of the Ericksen number Er; $Er < 0$ and $Er > 0$ mean flow from above or below, respectively.

We have solved the complete Ericksen–Leslie equations in the case of the dipolar configuration for arbitrary Ericksen numbers when $\boldsymbol{v}_\infty$ is directed along the dipole axis. This constitutes an effective two-dimensional problem. In figure 3 our results for the Stokes drag are illustrated. As abscissa coordinate we use the Ericksen number $Er \propto v_\infty$, where $Er > 0$ means flow from below, and $Er < 0$ means flow from above, as indicated by the inset in figure 3. The upper curve gives the distance r_d of the hyperbolic point defect from the centre of the sphere in units of the particle radius a. When the fluid flows from above ($Er < 0$), the defect is slightly pulled towards the sphere, and the distance r_d/a changes from 1.26 at $Er = 0$ to 1.13 at $Er = -30$. In the lower curve, we plot the Stokes drag $F_S^{\parallel}$ in terms of the effective viscosity $\eta^{\parallel}_{\rm eff} = F_S^{\parallel}/(6\pi a v_\infty)$. Corresponding to r_d, it also slightly decreases from 0.48 P at $Er = 0$ to 0.42 P at $Er = -30$. We understand this behaviour from an investigation of the director field (for figures, see [15]). Compared to the dipolar configuration in figure 1, the director field is straightened up along the vertical axis when the defect moves towards the particle. It is therefore more uniform, which reduces the resistance to flow. On the other hand, for $Er > 0$, the defect moves strongly away from the sphere which leads to a correspondingly strong increase of $\eta^{\parallel}_{\rm eff}$. Thus we can conclude that the Stokes drag in a nematic environment is not only anisotropic, but also behaves highly non-linearly. Furthermore, its magnitude crucially depends on whether the fluid first flows against the sphere ($Er < 0$) or against the point defect ($Er > 0$). Such a behaviour is only possible through the coupling between the velocity and the director field. It is due to the fact that the torque balance equation $\boldsymbol{n} \times (\boldsymbol{h}^{\rm el} - \boldsymbol{h}^{\rm visc}) = \boldsymbol{0}$ (see also equation (4)) is not invariant under $\boldsymbol{v} \to -\boldsymbol{v}$. In a static dipole configuration ($Er \to 0$), it therefore cannot occur. We also stress that the defect is not a solid object. Thus, the intuitive argument that the defect should be pushed against the particle for $Er > 0$ is not applicable here. The motion of the defect is solely determined by the non-trivial solution of the torque equation. A simple explanation for its behaviour is not obvious.

How realistic are high Ericksen numbers in a falling ball experiment? Balancing the gravitational, the buoyancy, and Stokes's friction force, we arrive at settling velocities for latex particles which give Ericksen numbers much smaller than one due to the small density mismatch. The mass density of gold particles, however, is larger by a factor of 20 than that of liquid crystals. Particles of radius 10 μm, $\eta_{\rm eff} = 0.5$ P, and $K = 10^{-6}$ dyn then give $Er = 5$. The settling velocity scales with a^2, so a variation of the Ericksen number is possible.

We conclude with a final remark. The point defect will not become detached from the droplet at a finite $Er > 0$, as figure 3 might suggest, since this costs too much elastic energy.

A more realistic scenario is that the defect becomes unstable for a large $Er > 0$, opens up to form a Saturn ring (as predicted for high magnetic or electric fields [1]), and possibly moves to a position above the particle that would correspond to $Er < 0$ in figure 3. However, due to a 'numerical pinning' of the defect ring, we are not able to verify this effect in a director theory [1]. We are currently working on an approach using the alignment tensor [11] to clarify this question.

Acknowledgment

HS acknowledges a generous financial support from a Heisenberg scholarship from the Deutsche Forschungsgemeinschaft.

References

[1] Stark H 2001 *Phys. Rep.* **351** 387
[2] Poulin P, Stark H, Lubensky T C and Weitz D A 1997 *Science* **275** 1770
[3] Meyer R B 1972 *Mol. Cryst. Liq. Cryst.* **16** 355
[4] Poulin P, Raghunathan V A, Richetti P and Roux D 1994 *J. Physique* II **4** 1557
[5] Terentjev E M 1995 *Phys. Rev.* E **51** 1330
[6] Borštnik A, Stark H and Žumer S 2000 *Phys. Rev.* E **61** 2831
Galatola P and Fournier J B 2001 *Phys. Rev. Lett.* **87** 3915
Stark H 2002 *Phys. Rev.* E **66** 041705
[7] Loudet J-C, Barois P and Poulin P 2000 *Nature* **407** 611
[8] Meeker S P, Poon W C K, Crain J and Terentjev E M 2000 *Phys. Rev.* E **61** R6083
[9] Nazarenko V G, Nych A B and Lev B I 2001 *Phys. Rev. Lett.* **87** 075504
[10] Yamamoto R 2001 *Phys. Rev. Lett.* **87** 075502
[11] Fukuda J, Yoneya M and Yokoyama H 2002 *Phys. Rev.* E **65** 041709
[12] Good K, Care C M, Halliday I and Cleaver D J in preparation
[13] Ruhwandl R W and Terentjev E M 1996 *Phys. Rev.* E **54** 5204
[14] Stark H and Ventzki D 2001 *Phys. Rev.* E **64** 031711
[15] Stark H and Ventzki D 2002 *Europhys. Lett.* **57** 60
[16] Brenner H 1963 *Chem. Eng. Sci.* **18** 1
Brenner H 1964 *Chem. Eng. Sci.* **19** 599
[17] Russel W B, Saville D A and Schowalter W R 1995 *Colloidal Dispersions* (Cambridge: Cambridge University Press)
[18] Chandrasekhar S 1992 *Liquid Crystals* 2nd edn (Cambridge: Cambridge University Press)
[19] de Gennes P G and Prost J 1993 *The Physics of Liquid Crystals* 2nd edn (Oxford: Oxford Science Publications)
[20] Mięsowicz M 1935 *Nature* **136** 261
Mięsowicz M 1946 *Nature* **158** 27
[21] Stark H, Lubensky T and Yan G in preparation
[22] Sommerfeld A 1978 *Vorlesungen Über Theoretische Physik II. Mechanik der Deformierbaren Medien* 6th edn (Frankfurt: Deutsch)
[23] Lubensky T C, Pettey D, Currier N and Stark H 1998 *Phys. Rev.* E **57** 610